Cost of cone coupling to trichromacy in primate fovea

Andrew Hsu and Robert G. Smith

Department of Neuroscience, University of Pennsylvania, Philadelphia, Pennsylvania 19104

Gershon Buchsbaum

Department of Bioengineering, University of Pennsylvania, Philadelphia, Pennsylvania 19104

Peter Sterling

Department of Neuroscience, University of Pennsylvania, Philadelphia, Pennsylvania 19104

Received June 28, 1999; revised manuscript received November 11, 1999; accepted November 17, 1999

Cone synaptic terminals couple electrically to their neighbors. This reduces the amplitude of temporally uncorrelated voltage differences between neighbors. For an achromatic stimulus coarser than the cone mosaic, the uncorrelated voltage difference between neighbors represents mostly noise; so noise is reduced more than the signal. Here coupling improves signal-to-noise ratio and enhances contrast sensitivity. But for a chromatic stimulus the uncorrelated voltage difference between neighbors of different spectral type represents mostly signal; so signal would be reduced more than the noise. This cost of cone coupling to encoding chromatic signals was evaluated using a compartmental model of the foveal cone array. When cones sensitive to middle (M) and long (L) wavelengths alternated regularly, and the conductance between a cone and all of its immediate neighbors was 1000 pS (~2 connexons/cone pair), coupling reduced the difference between the L and M action spectra by nearly fivefold, from about 38% to 8%. However, L and M cones distribute randomly in the mosaic, forming small patches of like type, and within a patch the responses to a chromatic stimulus are correlated. In such a mosaic, coupling still reduced the difference between the L and M action spectra, but only by 2.4-fold, to about 18%. This result is independent of the L/M ratio. Thus "patchiness" of the L/M mosaic allows cone coupling to improve achromatic contrast sensitivity while minimizing the cost to chromatic sensitivity. [S0740-3232(00)02103-7]

OCIS codes: 330.0330, 330.1720, 330.4060, 330.4270, 330.5310, 330.5510, 330.6180.

1. INTRODUCTION

At the first stage in retinal circuitry the synaptic terminals of neighboring cones form gap junctions that couple them electrically. Cone coupling occurs, not only in lower vertebrates, where it was first described (e.g., Refs. 1–3), but also in mammals (e.g., in Refs. 4 and 5). Gap junctions are even present between cone terminals in primate fovea.[6,7] This seems counterintuitive: we can perceive an image as fine as the foveal cone mosaic; yet coupling the elements of this mosaic would reduce their voltage differences and thus blur the image.

But the gap junctions between foveal cones are small,[6–8] and the blur that they cause is calculated to be less than the blur caused by the eye's optics. This modest reduction of voltage differences between cones is advantageous when a stimulus is coarser than the cone mosaic. Then signals in adjacent cones are temporally correlated, so their voltage differences due to signal are small; this minimizes spread of the signal and preserves its amplitude. But noises in adjacent cones are temporally uncorrelated, so their voltage differences are large; this maximizes spread of the noise and strongly reduces its amplitude. This increases signal-to-noise ratio and thus improves achromatic contrast sensitivity.[2,3,8]

However, cone coupling raises a difficulty for color vision. When a chromatic stimulus coarser than the cone mosaic evokes a voltage difference in adjacent cones of different spectral type, coupling will reduce the difference and effectively shift their action spectra closer together. This will tend to reduce chromatic sensitivity. We asked for primate fovea how large this effect would be and how strongly it would depend on the structure of the cone mosaic. To address these questions we constructed a compartmental model of the foveal cone array for which we could specify spectral sensitivity of the three cone types, their distributions in the array, and their coupling strengths.

2. METHODS

A. Model

A compartmental model of a 16 × 16 foveal cone array was constructed using the NeuronC simulator.[9] Each cone consisted of a light-sensitive outer segment conductance (1 nS), a passive inner segment conductance (1 nS), and standard electrical compartments corresponding to the passive electrical properties of the long, thick axon (380 μm, 1.6-μm diameter) and the large synaptic terminal (7-μm diameter). Cone input resistance was approximately 0.5 GΩ, in agreement with calculated input resis-

tance in monkey cones.[10] The model assumed that $R_m = 50\,\mathrm{k\Omega/cm^2}$,[11] $R_i = 200/\Omega\,\mathrm{cm}$,[12,13] and $C_m = 1\,\mu\mathrm{F/cm^2}$.[14] Further detail regarding the geometry and electrical properties of the cone model are given by Hsu *et al.*[15] and by Smith.[9]

A flash decreased the simulated outer segment conductance linearly with intensity (Fig. 1), and the response was scaled for each cone type [short, middle, or long (S, M, or L) wavelength] according to the spectral sensitivity curves measured in isolated monkey cones [Fig. 2(a)].[16] Since the simulations were to be compared with the action spectra of isolated cones, we omitted preneural factors such as losses due to absorption by lens, ocular media, and macular pigment. The ratio of cone types was typically 10S:45M:45L.[17,18] S cones were spaced regularly, and various arrangements were tested for L and M cones. Although the S cone distribution is not perfectly regular in primate retina,[17] the key feature for present purposes is that S cones are rarely, if ever, nearest neighbors. We tested L and M cones arranged in regularly alternating and random sequences. The latter were constructed by choosing L and M cones from a uniform probability distribution based on their ratio.

B. Action Spectra

Action spectra were determined by presenting monochromatic flashes to the entire cone array [1 ms; 1×10^4 (photons/μm^2)/s] at wavelengths between 380 and 700 nm in 5-nm steps. To identify the wavelength of peak sensitivity for L and M cones, flashes were presented between 530 and 560 nm in 0.5-nm steps. In both simulations, the peak photovoltage was measured at the cone synaptic terminal 60 ms after flash onset. Responses for each cone type were then averaged and normalized to the peak sensitivity of an uncoupled cone of the same type. The procedure was repeated to cover the entire range of wavelengths. For random arrays, action spectra from five different arrays (with identical parameters) were averaged to ensure that the result was not due to a particular arrangement of cones.

C. Cone Coupling

The gap junction is a supramolecular structure recognized by conventional electron microscopy as a region

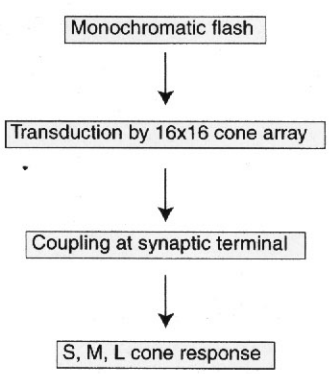

Fig. 1. Diagram of the simulation. Each cone responded with a photovoltage according to the action spectrum defined by its S, M, or L pigment. The voltages were then pooled by electrical coupling at the synaptic terminal. Responses were measured separately for each cone, then averaged for cones of like type.

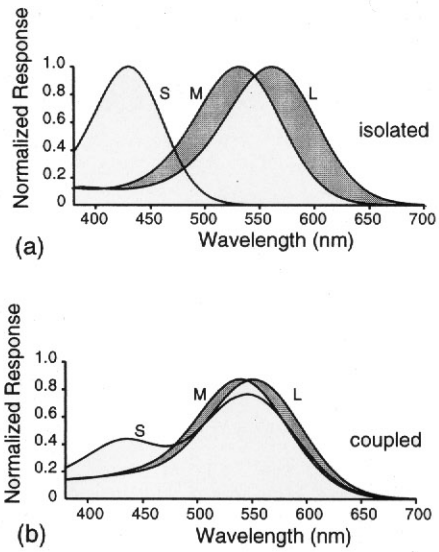

Fig. 2. Cone coupling shifts action spectra. (a) Action spectra of isolated S, M, and L cones from Ref. 1. Shading indicates area of nonoverlap between L and M spectra [plotted in Figs. 4(a) and 5(a) below]. (b) Action spectra with 1000-pS coupling conductance. Shading, same as in (b).

where two membranes are closely opposed (reviewed in Ref. 19). This apposition reflects a focal accumulation of intercellular channels termed "connexons." The connexon is in effect a donut comprising six protein subunits, termed "connexins," which comprise a diverse family of more than a dozen isoforms.[19] The conductance is specific for each connexin isoform, but ranges from about 50 to 150 pS.[19] Which connexin is expressed at the primate cone terminal is unknown, so we adopted a middle value of 100 pS. However, the critical value is not this unitary conductance but rather the total conductance between each cone and its neighbors. That value is constrained in the model so that the electrical spread is less than the known optical spread (see Section 3).

3. RESULTS

A. Dependence of Signal Spread on Coupling

We simulated a cone array with each cone coupled equally to its four nearest neighbors.[7] The coupled cones form a resistive network that filters the voltage response of each cone. The filtering is simply a linear convolution of the cone voltages with the spread function of the resistive network. In a two-dimensional resistive grid, this is a modified Bessel function of the second kind, roughly exponential.[2] Its dependence on coupling can be estimated simply in a one-dimensional array, where it is nearly exponential:

$$y(x) = \exp(-|x/\lambda|), \tag{1}$$

where x is the distance in cone diameters from a central cone; λ is the space constant computed from

$$\lambda = \left(\frac{\text{cone input resistance}}{\text{coupling resistance}}\right)^{1/2}. \tag{2}$$

With a cone input resistance of 0.5 GΩ and a coupling resistance of 1 GΩ (corresponding to 10 connexons at 100

pS/connexon), the space constant is about 0.7 cone diameters. This value of coupling resistance was chosen for several reasons. First, at about two connexons per cone pair, coupling is almost irreducibly weak, that is, if the number of connexons were set lower by a factor of 2, the model would reduce to the uncoupled case. Second, patch clamp recordings from pairs of adjacent cones (ground squirrel) show coupling of this order.[20] Third, stronger coupling would cause the space constant to exceed the optical blur. This would reduce spatial acuity below what has been psychophysically determined.[21] In short, coupling resistance is constrained at the low end by the null condition and at the high end by known performance.

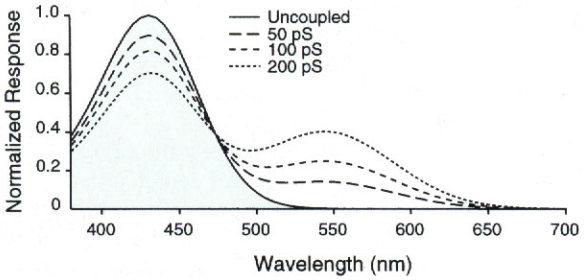

Fig. 3. Even modest coupling of S cone markedly shifts its action spectrum. S cone coupling varied between 0 and 200 pS; M and L cone coupling was constant at 1000 pS.

B. Effect of Coupling on Cone Action Spectra

In a random array, coupling at 1000 pS alters the action spectra of all three cone types [Fig. 2(b)]. S cone sensitivity at short wavelengths is drastically reduced; the peak is shifted from 430 to about 435 nm, and a second peak appears at longer wavelengths. L and M cone sensitivities are also reduced, and the peaks of their action spectra shift toward each other.

So marked was the effect of 1000-pS coupling on the S cone action spectrum that we considered smaller conductances. S cone terminals, identified in electron micrographs by their contacts with blue ON bipolar cells, do form gap junctions.[22] However, the lateral processes (where gap junctions form) are fewer and stubbier for S cone terminals than for L and M terminals.[23] Figure 3 shows that weaker coupling enhances the peak at shorter wavelengths and reduces the peak at longer wavelengths.

C. Effect of Coupling and Cone Packing Arrangement on L and M Action Spectra

The shaded region in Fig. 2(a) identifies the region of nonoverlap between L and M action spectra. The degree of nonoverlap was computed as

$$1 - (\text{shaded area/total area}). \quad (3)$$

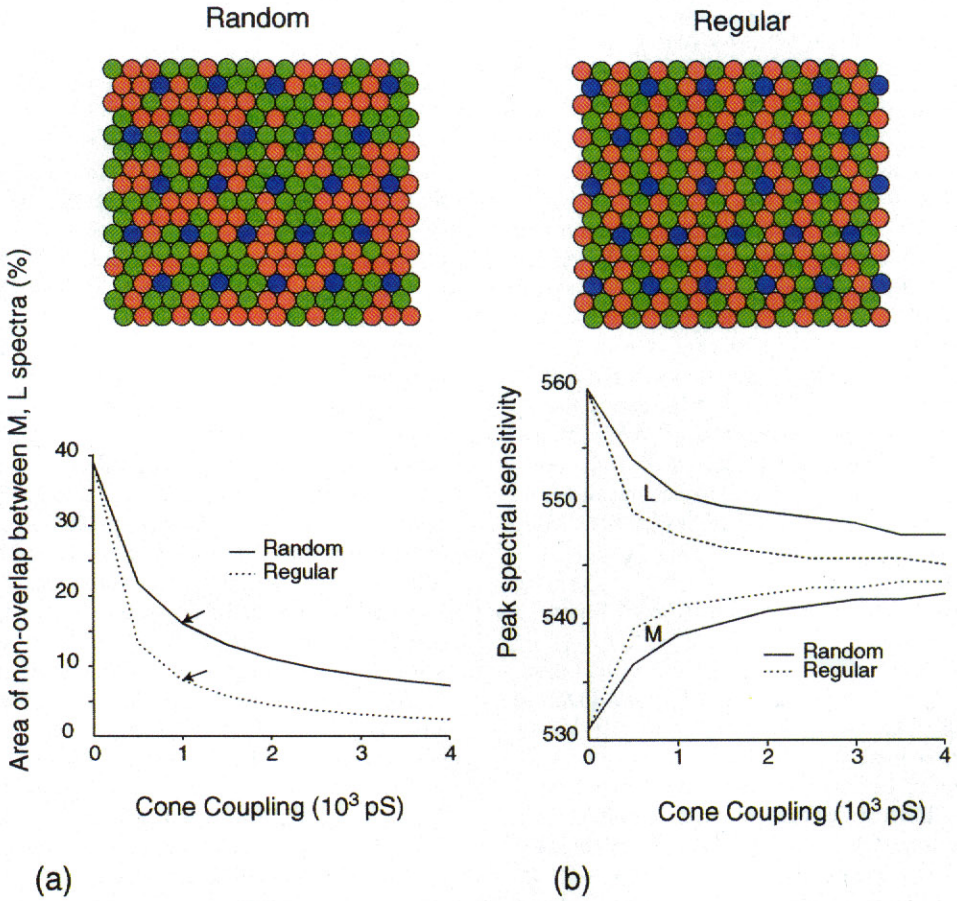

Fig. 4. Coupling reduces separation of L and M action spectra. (a) Reduction is greater for a regular (alternating) array than for a random array. For a coupling strength of 1000 pS (arrows), separation between L and M spectra is twofold larger for the random array than for the regular array. (b) With coupling, peak sensitivities for L and M cones converge toward 545 nm. Convergence is steeper for the regular array.

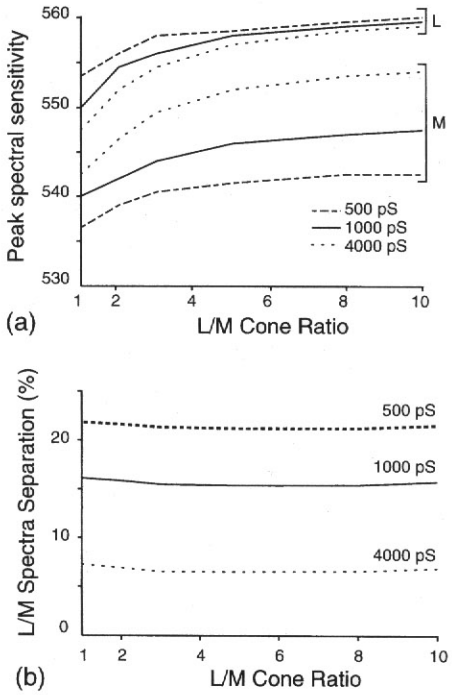

Fig. 5. L/M ratio in random array little affects separation of the action spectra or peak spectral sensitivities. (a) Area of nonoverlap for random array decreases with greater coupling, but cone ratio has no effect, except for slight dip at L/M = 3. (b) Peaks of L and M action spectra plotted against L/M ratio. Peaks for isolated L and M cones are, respectively, 530 and 560 nm; i.e., they are separated by 30 nm. As the L/M ratio rises, the L peak approaches that of the isolated cone, and the M peak asymptotes to an intermediate wavelength. Despite the shift, the distance between the peaks remains constant.

Without coupling, nonoverlap is nearly 40% [Figs. 2(a) and 4(a)]. Coupling sharply decreases the area of nonoverlap [Figs. 2(b) and 4(a)] with asymptote for coupling greater than 1000 pS. For an alternating arrangement of L and M cones, 1000-pS coupling reduces the area of nonoverlap to about 8%. For a random arrangement the reduction is only half that, about 16% [Fig. 4(a)].

As coupling increases, L and M cone peak sensitivities converge toward 545 nm [Fig. 4(b)]. The steepness of this convergence and its dependence on cone arrangement are identical to the decreased separation of the action spectra. The L and M curves are identical because the simulated array contained equal numbers of both cone types.

D. L/M Cone Ratio Little Affects Separation of Their Action Spectra

The ratio of L to M cones was reported in Old World monkey fovea to be 1 (Refs. 18 and 24) and in human fovea to be about 2 (Ref. 25). However, new methods with larger samples show clearly that the L/M ratio varies markedly across the retina and between individuals.[26–29] Therefore we considered how the effect of coupling would vary for different L/M ratios. Figure 5(a) shows that the L/M ratio hardly affects the area of overlap between the L and M action spectra, and Fig. 5(b) shows why. As the proportion of L cones rises, peak sensitivity of the L cone asymptotes toward its uncoupled maximum (560 nm) because there is progressively less voltage difference between neighbors due to spectral difference. But, simultaneously the M cones become more surrounded by L cones, so their sensitivity asymptotes toward the case of strict alternation (Fig. 4). Thus, for all L/M ratios >3, the two curves remain parallel [Fig. 5(b)].

4. DISCUSSION

The first stage of neural processing pools signals from adjacent cones via electrical synapses. This preferentially reduces the amplitude of their voltage differences. Where the differences are mostly noise (due to photon fluctuation), pooling improves signal-to-noise ratio. This occurs for achromatic stimuli of low spatial frequency, for which coupling may improve contrast sensitivity by about 50%.[8]

But this improvement to achromatic vision implies a cost to color vision. A chromatic stimulus of low spatial frequency evokes voltage differences in adjacent cones due solely to their different spectral sensitivities. These differences represent, not noise, but rather the very signals that are critical for color vision. Consequently, cone coupling that improves achromatic signals must attenuate chromatic signals. Here, using a compartmental model of the cone array, we find that cone coupling must shift the S cone action spectrum toward longer wavelengths and shift the L and M cone action spectra closer together, reducing their area of nonoverlap.

These effects depend on the strength of coupling. That each cone contacts 4–5 neighbors is known from electron microscopy,[7] but the number of active connexons and their single channel conductances are unknown. Nevertheless, the main value used here, 1000 pS/cone, represents only about two connexons per cone pair. For this value, the voltage would spread with a space constant of only 0.7 cones, less than the optical point spread.[8] Thus the effects reported here are for coupling strengths that are almost irreducibly small.

An effect of electrical coupling on cone spectral sensitivity has been demonstrated experimentally in cone recordings from fragments of intact retina.[30] In these experiments the relative sensitivities of cones to 500- and 600-nm light shift from the values for isolated M and L cones toward the value for rods which form small gap junctions with cones (Fig. 5 in Ref. 30). The magnitude of this shift varied considerably within a cone type, and this variation might arise from coupling between cones. Variability should be expected from cone–cone coupling because a given M or L cone will connect to a variable number of the other type. Although the predicted shift of M and L cones toward 545 nm [Fig. 4(b)] was not observed,[30] it might have been had the rod component been suppressed by a prior bleach.

The effect of coupling on the S cone action spectrum is to cause a second hump at longer wavelengths [Figs. 2(b) and 3]. Although this spectrum looks weird compared with that of S opsin, psychophysical attempts to isolate the S cone action spectrum do show a modest second hump (π_1 mechanism; Fig. 2 in Ref. 31). This suggests that S cone signals pass through sites in retina where signals from other cone types can affect sensitivity.[31] One

possible site would be the electrical synapses between S cone and L and M cone terminals.

A. Random Array Protects Separation of Action Spectra

If L and M cones formed a regularly alternating array, coupling would reduce the separation of their action spectra by nearly fivefold. However, we now know that L and M cones form a patchy array, often statistically indistinguishable from random array.[26] Cones within a patch of like type generate no voltage difference due to spectral difference; therefore coupling will cause no spectral blur. This reduces the cost of coupling to trichromacy by about twofold and may explain the selective advantage of generating randomness in the array (Fig. 4). Given a patchy array and a specific degree of coupling, separation of the L and M action spectra is unaffected by the L/M ratio—which is fortunate since this ratio is highly variable.

B. Extent of the Spectral Shifts Due to Coupling

Variations of amino acid sequence in cone pigments produce spectrally variant subtypes of L and M cones. The action spectra can shift as much as 16 nm,[27] and the most common variant in human males with normal color vision shifts L cone sensitivity by 4–7 nm.[32] Since these shifts are similar in magnitude to the shifts in action spectra predicted for cone coupling (~10 nm), the precise location of spectral peaks may little affect normal human color vision.

5. CONCLUSION

For spatial vision, the cost of trichromacy appears to be minor and may be revealed only in specialized circumstances.[33] For example, upon viewing a fine achromatic grating, blotches of unsaturated color are seen at lower frequency than the grating itself. These "Brewster colors" have been attributed to chromatic aliasing.[33] The cost to spatial vision of using different cone types is minimized because the M and L cones responsible for 90–95% of the spatial sampling have greatly overlapping action spectra; therefore both cone types can serve the same spatial sampling array. For trichromatic vision the cost of coupling cones to improve spatial vision also appears to be minor because the resultant blurring of the action spectra is reduced by distributing the M and L cones in patches.

ACKNOWLEDGMENTS

This research was supported by grants EY08124 and MH48168 from the National Institutes of Health. We thank Ed Pugh for comments on the manuscript and Sharron Fina for preparing it.

P. Sterling can be reached by e-mail at peter @retina.anatomy.upenn.edu.

REFERENCES AND NOTES

1. D. A. Baylor, M. G. F. Fuortes, and P. M. O'Bryan, "Receptive fields of cones in the retina of the turtle," J. Physiol. (London) **214**, 265–294 (1971).
2. T. D. Lamb and E. J. Simon, "The relation between intercellular coupling and electrical noise in turtle photoreceptors," J. Physiol. (London) **263**, 257–286 (1976).
3. M. Tessier-Lavigne and D. Attwell, "The effect of photoreceptor coupling and synapse nonlinearity on signal: noise ratio in early visual processing," Proc. R. Soc. London Ser. B. **234**, 171–197 (1988).
4. H. Kolb, "The organization of the outer plexiform layer in the retina of the cat: electron microscopic observations," J. Neurocytol. **6**, 131–153 (1977).
5. P. Sterling, M. A. Freed, and R. G. Smith, "Architecture of the rod and cone circuits to the *On*-beta ganglion cell," J. Neurosci. **8**, 623–642 (1988).
6. E. Raviola and N. B. Gilula, "Gap junctions between photoreceptor cells in the vertebrate retina," Proc. Natl. Acad. Sci. USA **70**, 1677–1681 (1973).
7. Y. Tsukamoto, P. Masarachia, S. J. Schein, and P. Sterling, "Gap junctions between the pedicles of macaque foveal cones," Vision Res. **32**, 1809–1815 (1992).
8. A. Hsu, L. Hahn, G. Buchsbaum, and P. Sterling are preparing a manuscript entitled, "Why cones in the human fovea are electrically coupled."
9. R. G. Smith, "NeuronC: a computational language for investigating functional architecture of neural circuits," J. Neurosci. Methods **43**, 83–108 (1992).
10. D. M. Schneeweis and J. L. Schnapf, "Photovoltage of rods and cones in the macaque retina," Science **268**, 1053–1056 (1995).
11. D. Johnston and T. H. Brown, "Interpretation of voltage-clamp measurements in hippocampal neurons," J. Neurophysiol. **50**, 464–486 (1983).
12. D. Attwell, F. S. Werblin, and M. Wilson, "The properties of single cones isolated from the tiger salamander retina," J. Physiol. (London) **328**, 259–283 (1982).
13. E. M. Lasater, R. A. Normann, and H. Kolb, "Signal integration at the pedicle of turtle cone photoreceptors: an anatomical and electrophysiological study," Visual Neurosci. **2**, 553–564 (1989).
14. J. J. B. Jack, D. Noble, and R. W. Tsien, *Electric Current Flow in Excitable Cells* (Clarendon, Oxford, UK, 1988).
15. A. Hsu, Y. Tsukamoto, R. G. Smith, and P. Sterling, "Functional architecture of primate rod and cone axons," Vision Res. **38**, 2539–2549 (1998).
16. D. A. Baylor, B. J. Nunn, and J. L. Schnapf, "Spectral sensitivity of cones of the monkey *Macaca fascicularis*," J. Physiol. (London) **390**, 145–160 (1987).
17. C. A. Curcio, K. A. Allen, K. R. Sloan, C. L. Lerea, J. B. Hurley, I. B. Klock, and A. H. Milam, "Distribution and morphology of human cone photoreceptors stained with anti-blue opsin," J. Comp. Neurol. **312**, 610–624 (1991).
18. J. D. Mollon and J. K. Bowmaker, "The spatial arrangement of cones in the primate fovea," Nature **360**, 677–679 (1992).
19. D. C. Spray, E. Scemes, and R. Rozental, in *Fundamental Neuroscience*, M. Zigmond, F. E. Bloom, S. C. Landis, J. L. Roberts, and L. R. Squire, eds. (Academic, San Diego, Calif., 1999), pp. 317–343.
20. S. H. De Vries, Houston Medical School, University of Texas, Houston, Tex. 77030 (personal communication, 1999).
21. N. Sekiguchi, D. R. Williams, and D. H. Brainard, "Efficiency in detection of isoluminant and isochromatic interference fringes," J. Opt. Soc. Am. A **10**, 2118–2133 (1993).
22. D. J. Calkins, Y. Tsukamoto, and P. Sterling, "Microcircuitry and mosaic of a blue/yellow ganglion cell in the primate retina," J. Neurosci. **18**, 3373–3385 (1998).
23. P. Ahnelt, C. Keri, and H. Kolb, "Identification of pedicles of putative blue-sensitive cones in the human retina," J. Comp. Neurol. **293**, 39–53 (1990).
24. D. J. Calkins, S. Schein, Y. Tsukamoto, and P. Sterling, "M and L cones in macaque fovea connect to midget ganglion cells via different numbers of excitatory synapses," Nature **371**, 70–72 (1994).
25. C. M. Cicerone and J. L. Nerger, "The relative numbers of long-wavelength-sensitive to middle-wavelength-sensitive

cones in the human fovea centralis," Vision Res. **29**, 115–128 (1989).
26. A. Roorda and D. R. Williams, "The arrangement of the three cone classes in the living human eye," Nature **397**, 520–522 (1999).
27. M. Neitz, J. Neitz, and G. H. Jacobs, "Spectral tuning of pigments underlying red–green color vision," Science **252**, 971–974 (1991).
28. S. B. Balding, S. A. Sjoberg, M. Neitz, and J. Neitz, "Real time PCR method to accurately quantitate L and M cone pigment gene expression," Invest. Ophthalmol. Visual Sci. Suppl. **39**, 959 (1998).
29. S. A. Hagstrom, J. Neitz, and M. Neitz, "Variations in cone populations for red–green color vision examined by analysis of mRNA," NeuroReport **9**, 1963–1967 (1998).
30. D. M. Schneeweis and J. L. Schnapf, "The photovoltage of macaque cone photoreceptors: adaptation, noise, and kinetics," J. Neurosci. **19**, 1203–1216 (1999).
31. E. N. Pugh, Jr., and J. D. Mollon, "A theory of the π_1 and π_3 color mechanisms of Stiles," Vision Res. **19**, 293–312 (1979).
32. T. W. Kraft, J. Neitz, and M. Neitz, "Spectra of human L cones," Vision Res. **38**, 3663–3670 (1998).
33. D. R. Williams, N. Sekiguchi, W. Haake, D. Brainard, and O. Packer, in *From Pigments to Perception*, A. Valberg and B. B. Lee, eds. (Plenum, New York, 1991), pp. 11–22.